Mechanistic Aspects of Samarium-Mediated σ-Bond Activations of Arene C−H and Arylsilane Si−C Bonds

Ivan Castillo and T. Don Tilley*

Contribution from the Department of Chemistry, University of California at Berkeley, Berkeley, California 94720-1460

Received June 15, 2001

Abstract: To investigate the potential role of Sm−Ph species as intermediates in the samarium-catalyzed redistribution of $PhSiH_3$ to Ph_2SiH_2 and SiH_4, the samarium phenyl complex $[Cp^*_2SmPh]_2$ (**1**) was prepared by oxidation of Cp^*_2Sm (**2**) with $HgPh_2$. Compound **1** thermally decomposes to yield benzene and the phenylene-bridged disamarium complex $Cp^*_2Sm(\mu\text{-}1,4\text{-}C_6H_4)SmCp^*_2$ (**3**). This decomposition reaction appears to proceed through dissociation of **1** into monomeric Cp^*_2SmPh species which then react via unimolecular and bimolecular pathways, involving rate-limiting Cp* metalation and direct C−H activation, respectively. The observed rate law for this process is of the form: rate $= k_1[\mathbf{1}] + k_2[\mathbf{1}]^2$. Complex **1** efficiently transfers its phenyl group to $PhSiH_3$, with formation of Ph_2SiH_2 and $[Cp^*_2Sm(\mu\text{-}H)]_2$ (**4**). Quantitative Si−C bond cleavage of $C_6F_5SiH_3$ is effected by the samarium hydride complex **4**, yielding silane and $[Cp^*_2Sm(\mu\text{-}C_6F_5)]_2$ (**5**). In contrast, Si−H activation takes place upon reaction of **4** with $o\text{-}MeOC_6H_4SiH_3$, affording the samarium silyl species $Cp^*_2SmSiH_2(o\text{-}MeOC_6H_4)$ (**7**). Complex **7** rapidly decomposes to $[Cp^*_2Sm(\mu\text{-}o\text{-}MeOC_6H_4)]_2$ (**6**) and other samarium-containing products. Compounds **5** and **6** were prepared independently by oxidation of **2** with $Hg(C_6F_5)_2$ and $Hg(o\text{-}MeOC_6H_4)_2$, respectively. The mechanism of samarium-mediated redistribution at silicon, and chemoselectivity in σ-bond metathesis reactions, are discussed.

Introduction

The activation of C−H[1,2] and Si−H[3] σ-bonds by f-element complexes is well established. On the other hand, related activations of C−C[2a,4] and Si−C[3f,5] bonds appear to be more difficult and have been observed far less often, with the former being limited to β-alkyl-transfer reactions. Several kinetic factors seem to favor C−H over C−C activation, including the inherently more hindered nature of C−C bonds, the statistical abundance of C−H bonds in most hydrocarbons, and the higher barrier for C−C activation due to its more directional bonding.[6] Nevertheless, remarkable examples of metal-mediated C−C bond activation by early transition metal centers have been reported by the group of Basset.[7] Such heterogeneous systems, which involve highly electrophilic, silica-supported early-transition metal centers, allow chemical transformations of hydrocarbons under mild conditions.

In metal−silicon chemistry, the analogous preference for Si−H over Si−C activation may be explained by the same factors recognized to account for chemoselectivity in C−H versus C−C activation. Thus, in reactions of d^0f^n metal hydrides with hydrosilanes, the usual reaction pathway involves dehydrocoupling via four-center transition state **A** and selective formation of a metal silyl derivative (Scheme 1). Such species have been invoked as intermediates in the dehydrocoupling of silanes, by way of reaction with more hydrosilane via transition state **B** to produce a Si−Si bond and regenerate the metal hydride. Thus, the first two reactions of Scheme 1 can account for the coordination−polymerization of organosilanes to polysilanes by early-transition metal and f-element complexes.[8]

The activation of Si−C bonds is potentially important in the development of new processes in organosilicon chemistry. In addition, studies of Si−C bond activations may provide important insights into designing comparable chemistry for C−C bonds, which is expected to be more difficult. Within this context, we have observed Si−C bond activation in samarium-

(1) For example: (a) Watson, P. L. *J. Am. Chem. Soc.* **1983**, *105*, 6491. (b) Jeske, G.; Lauke, H.; Mauermann, H.; Schumann, H.; Marks, T. J. *J. Am. Chem. Soc.* **1985**, *107*, 8111. (c) Bruno, J. W.; Smith, G. M.; Marks, T. J.; Fair, C. K.; Schultz, A. J.; Williams, J. M. *J. Am. Chem. Soc.* **1986**, *108*, 40. (d) Thompson, M. E.; Baxter, S. M.; Bulls, A. R.; Burger, B. J.; Nolan, M. C.; Santarsiero, B. D.; Schaefer, W. P.; Bercaw, J. E. *J. Am. Chem. Soc.* **1987**, *109*, 203.

(2) For reviews see: (a) Watson, P. L.; Parshall, G. W. *Acc. Chem. Res.* **1985**, *18*, 51. (b) Bercaw, J. E. *Pure Appl. Chem.* **1990**, *62*, 1151. (c) Davis, J. A., Watson, P. L., Liebman, J. F., Greenberg, A., Eds.; *Selective Hydrocarbon Activation*; VCH Publishers: New York, 1990. (d) Marks, T. J. *Acc. Chem. Res.* **1992**, *25*, 57.

(3) For example: (a) Forsyth, C. M.; Nolan, S. P.; Marks, T. J. *Organometallics* **1991**, *10*, 2543. (b) Sakakura, T.; Lautenschlager, H. J.; Nakajima, M.; Tanaka, M. *Chem. Lett.* **1991**, 913. (c) Tilley, T. D.; Radu, N. S.; Walzer, J. F.; Woo, H.-G. *Polym. Prepr. (Am. Chem. Soc., Div. Polym. Chem.)* **1992**, *33(1)*, 1237. (d) Molander, G. A.; Julius, M. *J. Org. Chem.* **1992**, *57*, 3266. (e) Radu, N. S.; Tilley, T. D. *J. Am. Chem. Soc.* **1995**, *117*, 5863. (f) Radu, N. S.; Hollander, F. J.; Tilley, T. D.; Rheingold, A. L. *J. Chem. Soc., Chem. Commun.* **1996**, 2459.

(4) (a) Watson, P. L.; Roe, D. C. *J. Am. Chem. Soc.* **1982**, *104*, 6471. (b) Bunel, E.; Burger, B. J.; Bercaw, J. E. *J. Am. Chem. Soc.* **1988**, *110*, 976.

(5) (a) Radu, N. S.; Tilley, T. D.; Rheingold, A. L. *J. Organomet. Chem.* **1996**, *516*, 41. (b) Castillo, I.; Tilley, T. D. *Organometallics* **2000**, *19*, 4733.

(6) (a) Crabtree, R. H. *Chem. Rev.* **1985**, *85*, 245 and references therein. (b) Rybtchinski, B.; Milstein, D. *Angew. Chem., Int. Ed.* **1999**, *38*, 870.

(7) For example: (a) Lecuyer, C.; Quignard, F.; Choplin, A.; Olivier, D.; Basset, J.-M. *Angew. Chem., Int. Ed.* **1991**, *30*, 1660. (b) Rosier, C.; Niccolai, G. P.; Basset, J.-M. *J. Am. Chem. Soc.* **1997**, *119*, 12408. (c) Maury, O.; Lefort, L.; Vidal, V.; Thivolle-Cazat, J.; Basset, J.-M. *Angew. Chem., Intl. Ed.* **1999**, *38*, 1952. (d) Chabanas, M.; Vidal, V.; Copéret, C.; Thivolle-Cazat, J.; Basset, J.-M. *Angew. Chem., Int. Ed.* **2000**, *39*, 1962.

(8) (a) Woo, H.-G.; Tilley, T. D. *J. Am. Chem. Soc.* **1989**, *111*, 8043. (b) Woo, H.-G.; Heyn, R. H.; Tilley, T. D. *J. Am. Chem. Soc.* **1992**, *114*, 5698. (c) Woo, H.-G.; Walzer, J. F.; Tilley, T. D. *J. Am. Chem. Soc.* **1992**, *114*, 7047. (d) Tilley, T. D. *Acc. Chem. Res.* **1993**, *26*, 22.

10.1021/ja011472w CCC: $20.00
Published on Web 10/05/2001

Scheme 1

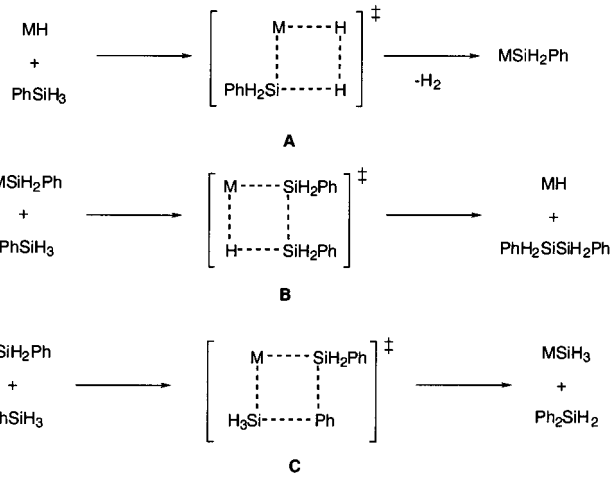

Scheme 2

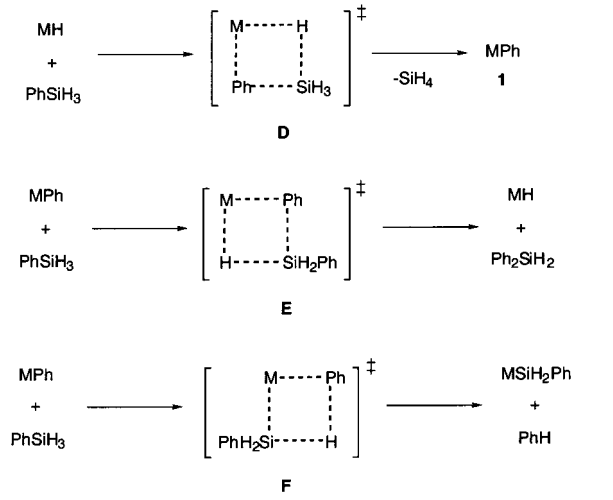

mediated conversions of phenylsilane to silane, benzene, diphenylsilane, and triphenylsilane, which strongly compete with the expected dehydrocoupling chemistry.[3f,5b] The Si−C activation could in principle occur via transfer of the phenyl group of $PhSiH_3$ to the metal-bound silyl fragment through a similar four-centered transition state (**C**, Scheme 1). The pathway involving transition state **C**, however, seems unlikely for both steric and electronic reasons. Addition of a M−Si bond to the Si−C bond of an organosilane produces an inherently crowded transition state.[3e] In addition, theoretical studies indicate that transition states with a carbon atom in the β-position are disfavored.[9]

An alternative mechanism for Si−C bond activation involves initial cleavage of the Si−C bond of phenylsilane via transition state **D** (Scheme 2), yielding silane and a metal−phenyl species. Arylation of $PhSiH_3$ by M−Ph (**E**, Scheme 2) could account for Ph_2SiH_2 formation, whereas protonation of M−Ph (**F**, Scheme 2) could result in the production of benzene.

In light of the scarcity of well-defined examples of Si−C σ-bond activation, and the potential relevance of this process to related C−C bond activation with electrophilic early-transition and f-element complexes, we have investigated mechanistic aspects of the $Cp^*_2SmR/PhSiH_3$ (R = H, alkyl) reaction system. A primary objective has been to identify fundamental processes for the activation of Si−C (and other relatively inert) bonds. Furthermore, it is of interest to establish factors that control selectivity in reactions of electrophilic lanthanide complexes with organosilanes (e.g., Si−C vs Si−H bond activation), and their potential relevance to analogous processes involving hydrocarbons.

Results and Discussion

In the samarium-catalyzed redistribution of $PhSiH_3$ to SiH_4, Ph_2SiH_2, and Ph_3SiH, a possible intermediate is the phenyl derivative Cp^*_2SmPh (**1**, Scheme 2). To explore the possible role of **1** in this chemistry, we sought to prepare and isolate this species. The characterization of **1** in solution by ^1H NMR spectroscopy was reported by Evans and co-workers, and this complex was isolated as its THF adduct $Cp^*_2SmPh(THF)$.[10] A synthetic procedure that circumvents the use of ethereal solvents that could potentially coordinate to the samarium center comprises oxidation of divalent Cp^*_2Sm (**2**) by diphenylmercury.[11] In cyclohexane-d_{12}, orange-red solutions of **1** were obtained in quantitative yield, as indicated by ^1H NMR spectroscopy (eq 1). Attempts to isolate **1** that had been prepared in pentane or benzene, however, led to low and variable yields (0−37%). When the synthesis of **1** was attempted in toluene, reaction with the solvent led to the isolation of $Cp^*_2SmCH_2Ph$.[12] Predominant activation of the benzylic C−H bond of toluene has previously been observed with related Y, La, and Ce systems.[13]

$$Cp^*_2Sm + {}^1/_2HgPh_2 \xrightarrow[-{}^1/_2Hg^0]{} {}^1/_2[Cp^*_2SmPh]_2 \qquad (1)$$

Monitoring the reaction in eq 1 in cyclohexane-d_{12} by ^1H NMR spectroscopy revealed the slow and quantitative decomposition of **1** to benzene (0.5 equiv) and a samarium-containing compound giving rise to a single Cp* resonance at δ 1.16. Infrared spectroscopy revealed the presence of a low-energy ν_{CH} stretching band at 2712 cm^{-1}, suggesting an agostic interaction.[14] Storing samples of **1** in the dark did not inhibit this clean decomposition. Manipulation of **1** proved virtually impossible due to the fact that the thermal decomposition reaction occurs in the solid state as well, even at −35 °C, such that orange-red, crystalline **1** decomposes overnight under nitrogen to a tan microcrystalline material (**3**). Combustion analysis of the decomposition product of **1** is consistent with the formula $C_{23}H_{32}Sm$. On the basis of the spectroscopic evidence and the known analogous behavior of Cp^*_2LnPh complexes (Ln = Sc,[1d] Lu[15]), it was assumed that decomposition product **3** is the *p*-phenylene-bridged dimer $Cp^*_2Sm(\mu\text{-}1,4\text{-}C_6H_4)SmCp^*_2$, which does not give rise to aromatic resonances in the ^1H NMR spectrum due to the proximity of all phenylene protons to the paramagnetic Sm center. The tan complex **3** is less soluble than **1** in aliphatic hydrocarbons, allowing for the formation of X-ray quality crystals from concentrated cyclohexane-d_{12} solutions.

(9) (a) Steigerwald, M. L.; Goddard, W. A., III. *J. Am. Chem. Soc.* **1984**, *106*, 308. (b) Rappé, A. K. *Organometallics* **1990**, *9*, 466. (c) Folga, E.; Ziegler, T. *Can. J. Chem.* **1992**, *70*, 333. (d) Ustynyuk, Y. A.; Ustynyuk, L. Y.; Laikov, D. N.; Lunin, V. V. *J. Organomet. Chem.* **2000**, *597*, 182.

(10) (a) Evans, W. J.; Bloom, I.; Hunter, W. E.; Atwood, J. L. *Organometallics* **1985**, *4*, 112. (b) Evans, W. J.; Gonzales, S. L.; Ziller, J. W. *J. Am. Chem. Soc.* **1991**, *113*, 9880.

(11) We wish to thank Professor William J. Evans for suggesting the synthesis of **1** by the oxidation method described.

(12) Evans, W. J.; Ulibarri, T. A.; Ziller, J. W. *Organometallics* **1991**, *10*, 134.

(13) (a) Booij, M.; Meetsma, A.; Teuben, J. H. *Organometallics* **1991**, *10*, 3246. (b) Booij, M.; Deelman, B.-J.; Duchateau, R.; Postma, D. S.; Meetsma, A.; Teuben, J. H. *Organometallics* **1993**, *12*, 3531.

(14) Brookhart, M.; Green, M. L. H.; Wong, L. L. *Prog. Inorg. Chem.* **1988**, *26*, 1.

(15) Watson, P. L. *J. Chem. Soc., Chem. Commun.* **1983**, 276.

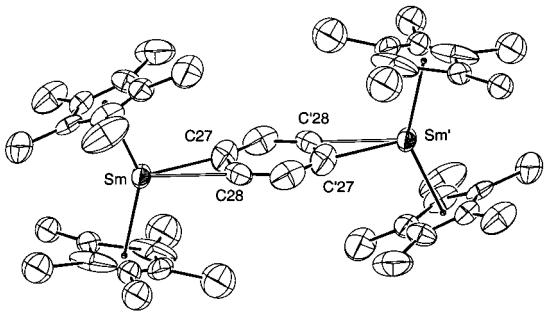

Figure 1. ORTEP view of $Cp^*_2Sm(\mu\text{-}C_6H_4)SmCp^*_2$ (**3**). The hollow lines represent the agostic interactions.

Compound **3** crystallizes in the monoclinic space group $P2_1/n$. Four $C_{23}H_{32}Sm$ fragments are contained in the unit cell, such that the asymmetric unit consists of one-half of the molecule including two Cp* rings, one samarium atom, and three carbon atoms from the bridging phenylene ligand. The other half of the molecule is related by an inversion center. One of the Cp* rings presents rotational disorder about the centroid−samarium vector, which was modeled as two superimposed Cp* groups (each with 50% occupancy) related by a rotation of approximately 36°.

A view of the molecular structure of **3** is provided in Figure 1. The $Sm-C_{ipso}$ distance of 2.42 Å is within the range of reported Sm−C σ-bonds for metallocene derivatives.[16] The Sm−Cp* centroid distance of 2.40 Å is also within the expected range for Sm(III) metallocenes,[16] although it is among the shortest, perhaps due to the electron deficient nature of **3**. The coordinative unsaturation of **3** is also evidenced by the presence of a β-agostic interaction involving ortho C−H bonds of the phenylene ligand. The Sm−C(28) distance of 2.79 Å involved in the agostic interaction is shorter than the sum of the van der Waals radii,[17] but significantly longer than the $Sm-C_{ipso}$ distance. The phenylene fragment is distorted by the β-agostic interaction, such that the $C_{ipso}-C'_{ipso}$ distance of 2.87 Å is elongated relative to the C(28)−C′(28) distance of 2.68 Å, and the $C_{ipso}-C'_{ipso}$ vector is at a 30.7° angle with respect to the $Sm-C_{ipso}$ bond vector. This type of β-H agostic interaction was observed for the analogous Lu complex, but not for the Sc one.[18] Finally, the wide centroid−Sm−centroid angle of 143.8° probably reflects the small steric demand of the phenylene unit. Table 1 summarizes the crystallographic data, and Table 2 provides selected bond distances and angles.

Reversibility of the Thermal Decomposition of 1 in Benzene. In cyclohexane-d_{12} solution, the formation of **3** is reversible, with the equilibrium lying toward the μ-phenylene complex (eq 2). Appreciable amounts of **1** were detected only when excess benzene was added to cyclohexane-d_{12} solutions of **3** (K_{eq} = 8.7 at 25 °C). In benzene-d_6 solution, **3** is quantitatively transformed into $Cp^*_2SmC_6D_5$ ($t_{1/2}$ = 0.25 h at 50 °C). Solutions of $Cp^*_2SmC_6D_5$ can also be prepared by dissolving **1** in benzene-d_6. This conversion is indicated by disappearance of the ^{1}H NMR resonances for the phenyl group of **1**, with concomitant formation of protiated benzene ($t_{1/2}$ = 0.50 h at 50 °C).

$$\underset{\mathbf{1}}{[Cp^*_2SmPh]_2} \rightleftharpoons \underset{\mathbf{3}}{Cp^*_2Sm(\mu\text{-}C_6H_4)SmCp^*_2} + PhH \quad (2)$$

(16) (a) Evans, W. J.; Foster, S. E. *J. Organomet. Chem.* **1992**, *433*, 79. (b) Schumann, H.; Meese-Marktscheffel, J. A.; Esser, L. *Chem. Rev.* **1995**, *95*, 865, and references therein.

(17) Emsley, J. *The Elements*; Oxford University Press: New York, 1990.

Table 1. Summary of Crystallographic Data

compound	**3**	**5**
formula	$C_{46}H_{64}Sm_2$	$C_{52}H_{60}F_{10}Sm_2$
MW	917.82	1175.82
cryst color, habit	tan, rodlike	red, rhomboidal
cryst dimens, mm	0.31 × 0.05 × 0.06	0.15 × 0.08 × 0.05
cryst system	monoclinic	triclinic
cell determination (2θ range)	2847 (4.0° − 45.0°)	3490 (4.0° − 45.0°)
lattice parameters		
a (Å)	8.6216(7	10.065(1)
b (Å)	21.143(1)	16.139(2)
c (Å)	11.9073(9)	17.323(2)
α (deg)		102.979(2)
β (deg)	β = 101.063(1)°	97.128(2)
γ (deg)		96.103(2)
V (Å^3)	2130.2(2)	2694.5(5)
space group	$P2_1/n$ (No. 14)	$P\bar{1}$(No. 2)
Z value	2	4
D_{calc} (g/cm^3)	1.431	1.449
μ(Mo Kα)	27.64 cm^{-1}	22.28 cm^{-1}
diffractometer	Siemens SMART	Siemens SMART
radiation	Mo−Kα	Mo−Kα
temperature (°C)	−123.0	−115.0
scan type	ω (0.3° per frame)	ω (0.3° per frame)
no. of reflns measd	10330	12182
no. of reflns obsd	1767 ($I > 3.00\sigma(I)$)	4685 ($I > 3.00\sigma(I)$)
solution	direct methods (SIR92)	direct methods (SIR92)
refinement	full-matrix least-squares	full-matrix least-squares
R; R_w	0.044; 0.050	0.040; 0.060
max peak in diff. map	0.95 e$^-$/Å^3	2.86 e$^-$/Å^3
min peak in diff. map	−0.68 e$^-$/Å^3	−0.53 e$^-$/Å^3

Table 2. Selected Bond Distances (Å) and Angles (deg) for **3**[a]

(a) Bond Distances

Sm	Cp*(1)	2.4030(7)	Sm	C(27)	2.42(2)
Sm	Cp*(2)	2.3965(7)	Sm	C(28)	2.79(2)

(b) Bond Angles

Cp*(1)	Sm	Cp*(2)	143.76(3)	Sm	C(27)	C(29)	152(1)
Sm	C(27)	C(28)	91(1)	C(28)	C(27)	C(29)	117(1)

[a] Cp* denotes the centroid of the ring.

Although compound **1** decomposes in pentane or toluene solution, as well as in the solid state, it is stable in benzene solution over a period of weeks. The stability of **1** in benzene allowed us to determine its solution molecular weight. By the Signer method,[19] **1** exists as a dimer in benzene. This result is consistent with the electrophilicity of the Sm center in **1,** and the fact that known metallocene hydrides and hydrocarbyls of the lanthanides are often dimeric with a bridging hydride or hydrocarbyl ligand.[1b,16,20] Unfortunately, the instability of **1** has precluded analysis of its solid-state structure by single-crystal X-ray diffraction studies.

Mechanism of the Decomposition of $[Cp^*_2SmPh]_2$ (1). To gain insight into the mechanism of C−H σ-bond activation in the decomposition of **1**, we monitored the reaction by ^{1}H NMR spectroscopy at 78 °C. Due to the instability of **1**, samples were prepared in methylcyclohexane-d_{14} immediately prior to each kinetic run. The experimental error in determining the concentration was estimated to be ≲10%.

At concentrations below 6.0 mM, plots of $\ln[\mathbf{1}]/[\mathbf{1}]_0$ versus time reflect the first-order disappearance of **1** (Figure 2). In all reactions, the rate of the formation of benzene was identical to

(18) Jahns, V.; Köstlmeier, S.; Kotzian, M.; Rösch, N.; Watson, P. L. *Int. J. Quantum Chem.* **1992**, *44*, 853.

(19) Zoellner, R. W. *J. Chem. Educ.* **1990**, *67*, 714.

(20) For example: (a) Watson, P. L.; Herskovitz, T. *ACS Symp. Ser.* **1983**, *212*, 459. (b) Stern, D.; Sabat, M.; Marks, T. J. *J. Am. Chem. Soc.* **1990**, *112*, 9558. (c) Haar, C. M.; Stern, C. L.; Marks, T. J. *Organometallics* **1996**, *15*, 1765.

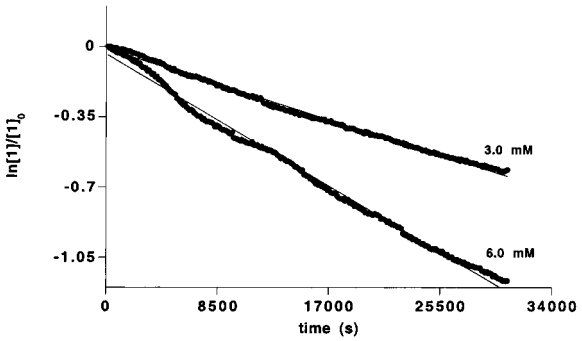

Figure 2. Kinetic plots for the apparent first-order disappearance of **1** (rate = k_{obs}[**1**]) at initial concentrations of 3.0 and 6.0 mM.

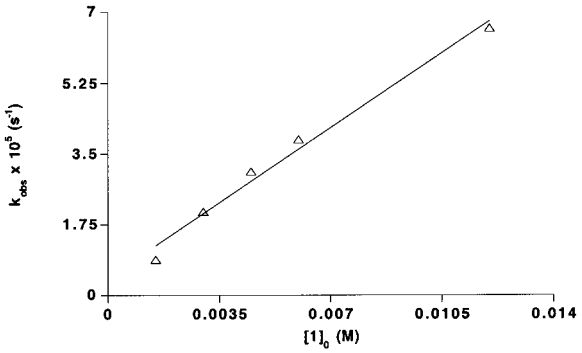

Figure 3. Plot of the values of k_{obs} with increasing [**1**]$_0$.

the rate of the disappearance of **1**. With an initial concentration of 6.0 mM, the decomposition reaction was kinetically well-behaved for 2 half-lives, indicating a rate law given by k_1[**1**]. Although the reactions involving lower initial concentrations of **1** (1.5−6.0 mM) seemed to also agree with first-order behavior, such kinetic runs revealed a dependence of the observed rate constant (k_{obs}) on [**1**]$_0$ (Figure 3). Thus, the reaction does not exhibit simple first-order behavior, and the rate behavior appears to be consistent with competing first- and second-order pathways (rate = k_1[**1**] + k_2[**1**]^2) with the first-order rate constant given by the *y*-intercept of Figure 3 (where [**1**]$_0$ = 0),[21] 4(1) × 10^{-6} s^{-1}. At the low initial concentrations of **1** examined, the second-order term is sufficiently small that the rearranged rate equation, rate = (k_1 + k_2[**1**])[**1**], can be described as k_{obs}[**1**], with k_{obs} = (k_1 + k_2[**1**]). The expression k_{obs}[**1**] gives rise to the apparent first-order behavior at such initial concentrations of **1** (1.5−6.0 mM).

When the initial concentration of **1** was raised to 12 mM, the kinetic behavior could be modeled reasonably by a second-order process, particularly early in the reaction, before [**1**] falls into the "first-order regime". At the high limit of initial concentration of **1** before insolubility becomes problematic (18 mM), the disappearance of **1** gives reasonable second-order plots to 50% conversion. Beyond 50% conversion, more complex rate behavior results from competing first- and second-order pathways. From the value of k_1 determined at low [**1**]$_0$ (Figure 3), it is possible to derive a value for k_2 by plotting exp[k_1t + ln([**1**]/[**1**]$_0$)] as a function of [**1**].[21] This method gives a linear plot with a slope = [k_2/(k_1 + k_2[**1**]$_0$)], from which a value of k_2 = 1(1) × 10^{-3} M^{-1} s^{-1} was extracted.

For determination of a kinetic isotope effect for the conversion of **1** to **3**, [Cp*$_2$SmC$_6$D$_5$]$_2$ was prepared from **2** and diphenylmercury-d_{10}. This allowed a determination of the kinetic isotope effect at low (6.0 mM) and high (18 mM) initial concentrations of [Cp*$_2$SmC$_6$D$_5$]$_2$. A small isotope effect k_H/k_D = 2.1(3) was obtained from the low-concentration runs, whereas a much larger value of k_H/k_D = 5.3(7) was obtained at high concentrations. The isotope effect obtained at low [**1**]$_0$ corresponds to the ratio of k_{obs} (with k_{obs} = k_1 + k_2[**1**], as described above) for the decomposition of [Cp*$_2$SmC$_6$H$_5$]$_2$ and [Cp*$_2$SmC$_6$D$_5$]$_2$, respectively. The isotope effect determined from the high [**1**]$_0$ kinetic runs, on the other hand, corresponds to the ratio of k_2's for the second-order disappearances of [Cp*$_2$SmC$_6$H$_5$]$_2$ and [Cp*$_2$SmC$_6$D$_5$]$_2$, respectively, since the bimolecular process k_2[**1**]^2 predominates at high initial concentrations of **1**. The observed isotope effect is therefore a function of the concentration of [Cp*$_2$SmC$_6$D$_5$]$_2$.

Competing first- and second-order kinetic behavior was previously observed in the related activations of benzene and benzene-d_6 by [Cp*$_2$LuMe]$_2$, which is a methyl-bridged dimer in equilibrium with the monomeric species Cp*$_2$LuMe.[1a] The equilibrium amount of monomeric Cp*$_2$LuMe in solution is apparently responsible for the activation of benzene. At low initial concentrations of benzene, a unimolecular reaction pathway involving rate-limiting metalation of the C−H bond of the Cp* ligand is associated with no kinetic isotope effect in the activation of benzene-d_6. This metalated species reacts rapidly with both benzene and benzene-d_6, resulting in no isotope effect. At high initial concentrations of benzene, a competing bimolecular reaction pathway was proposed to involve direct activation of a C−H or C−D bond of benzene or benzene-d_6 by Cp*$_2$LuMe in the transition state, resulting in a large isotope effect at higher concentrations of benzene-d_6 (where the bimolecular process predominates). The combination of the two processes gives rise to a concentration-dependent kinetic isotope effect.

A mechanism that is consistent with the observed rate behavior and the kinetic isotope effect in our system involves dimeric [Cp*$_2$SmPh]$_2$ in equilibrium with a monomeric species Cp*$_2$SmPh. The total concentration [**1**] therefore refers to the equilibrium mixture of monomer and dimer. Although we did not see evidence for more than one species in solution even at −80 °C, this can be expected if the monomer/dimer interconversion is fast even at low temperature. Rapid monomer/dimer equilibria in related f-element metallocene hydride and hydrocarbyl complexes have been described for a number of cases.[1a,b,20] In those systems, the monomeric species display enhanced σ-bond metathesis reactivity relative to their dimeric counterparts, as in the case of Cp*$_2$LuMe.[1a,20b,c,22] Therefore, it seems reasonable to assume that the equilibrium amount of Cp*$_2$SmPh present in solution might be more reactive toward σ-bond metathesis than [Cp*$_2$SmPh]$_2$. Decomposition of Cp*$_2$SmPh via activation of a C−H bond of one of the Cp* rings in the rate-limiting step would lead to loss of benzene and a metalated species which could rapidly react with another monomer of Cp*$_2$SmPh to produce **3** (**G** in Scheme 3). Such metalated species have been postulated as intermediates in hydrocarbon activation by early-transition and f-block metals.[1d,12,13,23] Decomposition of Cp*$_2$SmC$_6$D$_5$ by C−H activation of the Cp* ring in transition state **G** (Scheme 3) is consistent with the small kinetic isotope effect measured at low concentrations. At such low concentrations, the observed rate behavior can be modeled as a first-order process, associated with the unimolecular term k_1[**1**] in the rate equation.

(21) Espenson, J. H. *Chemical Kinetics and Reaction Mechanisms*; Series in Advanced Chemistry; McGraw-Hill: New York, 1981.

(22) Voskoboynikov, A. Z.; Parshina, I. N.; Shestakova, A. K.; Butin, K. P.; Beletskaya, I. P.; Kuz′mina, L. G.; Howard, J. A. K. *Organometallics* **1997**, *16*, 4041.

(23) Bulls, A. R.; Schaefer, W. P.; Serfas, M.; Bercaw, J. E. *Organometallics* **1987**, *6*, 1219.

Scheme 3

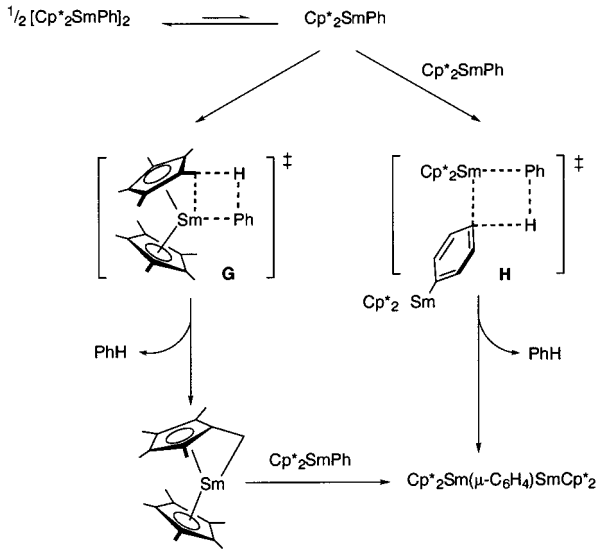

A decomposition route involving two Cp^*_2SmPh species could occur by activation of the C−H bond of one of the phenyl groups at the para position, with concomitant loss of benzene in the rate-limiting step (**H**, Scheme 3). This would give rise to second-order rate behavior at high concentrations of **1** with a bimolecular rate law $k_2[\mathbf{1}]^2$. The large kinetic isotope effect observed for the decomposition of $Cp^*_2SmC_6D_5$ at high initial concentration of **1** is consistent with C−D activation in transition state **H** (Scheme 3). At this time, we cannot completely rule out mechanisms involving reaction of monomeric Cp^*_2SmPh with the dimer, although such possibilities seem less consistent with the observed kinetic data.

Reaction of 1 with Phenylsilane. A key reaction in the postulated mechanism for the Sm-mediated redistribution of $PhSiH_3$ (Scheme 2) involves phenyl group transfer from samarium to silicon. To test for this possibility, we examined reactions of **1** with $PhSiH_3$. Samples of **1** were generated in cyclohexane-d_{12} solution. Addition of 1 equiv of $PhSiH_3$ to solutions of **1** at room temperature resulted in rapid conversion to products (phenylsilane was consumed before the ^{1}H NMR spectrum could be acquired). The observed products (80% Ph_2SiH_2 and 20% benzene as determined by ^{1}H NMR spectroscopy and GC−MS) are consistent with phenyl transfer to silicon. The phenylation of silicon by **1** results in an 80% conversion of the samarium species to $[Cp^*_2Sm(\mu\text{-}H)]_2$ (**4**), while the remaining 20% of the samarium-based products could not be accounted for by ^{1}H NMR spectroscopy.

Formation of 20% benzene in the reaction between **1** and $PhSiH_3$ is consistent with the pathway that goes through transition state **F** in Scheme 2. This result is also in agreement with our previous identification of benzene as a coproduct in the samarium-mediated redistribution at silicon.[5b] The mechanism for the production of Ph_2SiH_2 and benzene from samarium phenyl and $PhSiH_3$ is outlined in Scheme 4. Although the mechanism shown requires the formation of 20% $Cp^*_2SmSiH_2Ph$, it is reasonable that this samarium silyl complex would readily decompose to insoluble trisamarium clusters.[3f] An altenative explanation for the production of benzene from **1** involves direct hydrogenolysis with H_2. It is possible that dihydrogen could form by dehydrocoupling of $PhSiH_3$ with $Cp^*_2SmSiH_2Ph$, but on the basis of the small amount of Si−H relative to Si−C activation, we believe that this is a minor reaction pathway.

Reactions of $[Cp^*_2Sm(\mu\text{-}H)]_2$ (4) with Arylsilanes. A second, previously unobserved σ-bond metathesis step that is

Scheme 4

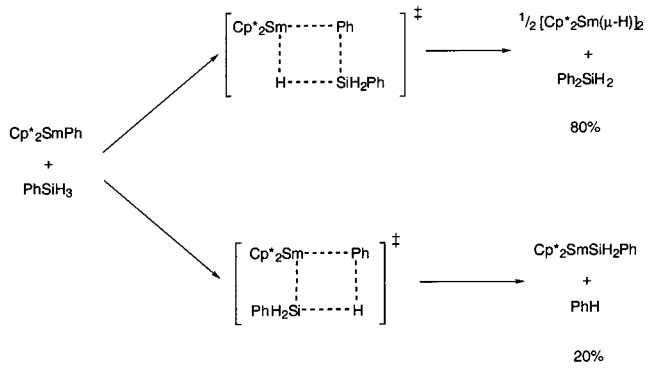

proposed in the redistribution of Scheme 2 involves cleavage of a Si−C(phenyl) bond by a samarium hydride. In the samarium-catalyzed redistribution of $PhSiH_3$, the phenyl derivative **1** was not observed as an intermediate. However, this is expected on the basis of the results described above, since any **1** produced during the reaction of **4** with $PhSiH_3$ would react rapidly with any phenylsilane still present in solution. Therefore, to directly observe a Si−C cleavage reaction (involving aryl transfer from silicon to samarium) we focused on reactions of **4** with arylsilanes that might produce a more stable (and observable) Sm−aryl product.

Previously, Andersen and Burns described the preparation of a perfluorophenyl derivative of ytterbocene which is quite stable.[24] Its enhanced stability undoubtedly results from the inductive effect of the fluorine atoms, which increase the anionic character of the Yb−C bond. This suggested that the silane $C_6F_5SiH_3$ might allow the direct observation of aryl transfer from silicon to samarium, with formation of a stable Sm−C_6F_5 complex. A second type of stabilized Sm−aryl derivative is suggested by the work of Teuben and co-workers in the synthesis of ortho-substituted yttrium−aryl complexes by C−H activation of the substituted arenes.[13b] Preference for activation of the ortho position was attributed to internal stabilization provided by coordination of a heteroatom lone pair to the metal center. Since activation of anisole proved to be the most facile,[13b] we also targeted the *o*-$MeOC_6H_4$− group for studies on aryl transfers.

A preparative procedure for $C_6F_5SiH_3$ was recently reported by the group of Molander.[25] We could not find reports on the synthesis of *o*-$MeOC_6H_4SiH_3$, but reduction of *o*-$MeOC_6H_4SiCl_3$[26] with $LiAlH_4$ provided the desired silane *o*-$MeOC_6H_4SiH_3$ as a colorless liquid after distillation.

To assess the stability of the targeted Sm−aryl complexes, they were prepared and isolated by independent syntheses that employed an oxidation method identical to that used for the synthesis of **1**. Thus, treatment of pentane slurries of **2** with 0.5 equiv of the corresponding diaryl mercury compounds afforded $[Cp^*_2Sm(\mu\text{-}C_6F_5)]_2$ (**5**) and $[Cp^*_2Sm(\mu\text{-}o\text{-}MeOC_6H_4)]_2$ (**6**) in good yields (eq 3). Compounds **5** and **6** are air- and moisture-sensitive but are stable in the solid state and in cyclohexane-d_{12} or benzene-d_6 solutions for at least one week.

$$\underset{\mathbf{2}}{Cp^*_2Sm} + {}^1/_2HgAr_2 \xrightarrow[-1/2Hg^0]{} {}^1/_2[Cp^*_2SmAr]_2 \qquad \begin{matrix} Ar = C_6F_5;\ \mathbf{5} \\ o\text{-}MeOC_6H_4;\ \mathbf{6} \end{matrix} \qquad (3)$$

(24) Burns, C. J.; Andersen, R. A. *J. Chem. Soc., Chem. Commun.* **1989**, 136.

(25) Molander, G. A.; Corrette, C. P. *Organometallics* **1998**, *17*, 5504.

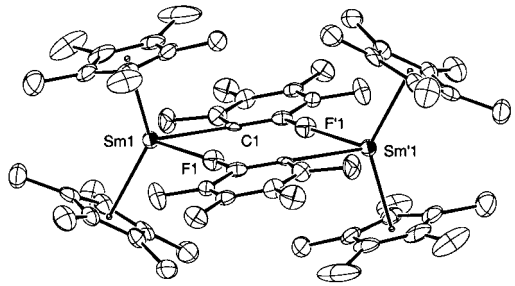

Figure 4. ORTEP diagram of $[Cp^*_2Sm(\mu\text{-}C_6F_5)]_2$ (**5**).

Table 3. Selected Bond Distances (Å) and Angles (deg) for **5**

(a) Bond Distances

Sm(1)	C(1)	2.60(1)	Sm(1)	Cp*(1)	2.4329(7)
Sm(2)	C(27)	2.60(1)	Sm(1)	Cp*(2)	2.4094(8)
Sm(1)	F(1)	2.531(8)	Sm(2)	Cp*(3)	2.4069(8)
Sm(2)	F(6)	2.539(7)	Sm(2)	Cp*(4)	2.4379(7)

(b) Bond Angles

F(1)	Sm(1)	C(1)	77.9(4)	Cp*(1)	Sm(1)	Cp*(2)	137.26(3)
F(6)	Sm(2)	C(27)	77.3(4)	Cp*(3)	Sm(2)	Cp*(4)	136.42(3)
Sm(1)	C(1)	C(2)	102.1(9)	Sm(2)	C(27)	C(28)	100.1(9)
Sm(1)	C(1)	C(6)	145(1)	Sm(2)	C(27)	C(32)	146(1)

[a] Cp* denotes the centroid of the ring.

The ^{1}H NMR spectrum of **5** displays a single resonance for the equivalent Cp* groups at δ 0.19, while that for **6** displays one Cp* resonance at δ 0.94 (30 H), four aromatic resonances (1 H each), and a paramagnetically shifted *Me*O resonance at δ −4.23 (3 H), indicative of the proximity of the methyl protons to the Sm center. Unfortunately, **6** crystallizes as very thin plates that were not suitable for single-crystal X-ray analysis. Thus, the mode of interaction of the *o*-methoxy group with the samarium atom could not be firmly established. A dimeric structure for **6** is proposed on the basis of the solution molecular weight obtained by the Signer method.

The ^{19}F NMR spectrum of **5** consists of three resonances in a 2:1:2 ratio. The resonance assigned to the ortho fluorine atoms is considerably broadened, indicating the presence of a Sm−F interaction. This was confirmed by analyzing the solid-state structure of **5**.

X-ray quality crystals of **5** were obtained by cooling concentrated pentane solutions to −35 °C. Compound **5** crystallizes in the triclinic space group $P\bar{1}$ with two independent monomers in the asymmetric unit that are related by an inversion center. The C_6F_5-groups bridge two samarium atoms through one ortho fluorine atom as shown in the ORTEP diagram of Figure 4. The two samarocene subunits are virtually identical, with average Cp* centroid−Sm distances of 2.42 Å and an average Cp*−Sm−Cp* angle of 136.9°. The Sm−C_{ipso} and Sm−F contacts are also identical for the two subunits, with values of 2.60 and 2.54 Å, respectively. Another feature of the solid-state structure is the proximity of a second set of ortho fluorine atoms to the Sm center, the distances being 2.85 and 2.82 Å between Sm(1)−F(2) and Sm(2)−F(10), respectively. A weak interaction between such atoms could provide a mechanism for the fluxional behavior of **5** in solution that gives rise to averaged fluorine resonances for the ortho and meta positions. The crystallographic data is summarized in Table 1, and selected bond distances and angles are provided in Table 3.

Reaction of the samarium hydride **4** with 1 equiv of $C_6F_5SiH_3$ in benzene-d_6 leads to the rapid and quantitative formation (by ^{1}H NMR spectroscopy) of **5** and SiH_4 (eq 4). Therefore, activation of the Si−C σ-bond of $C_6F_5SiH_3$ results in aryl-group transfer from silicon to samarium, with the formation of a stable Sm−aryl complex. Apparently, the strength of the Sm−C bond of **5** precludes further reaction, and no aryl transfer was observed from **5** to the silicon center of $C_6F_5SiH_3$ at room temperature after 24 h. Heating solutions of **5** and $C_6F_5SiH_3$ to 65 °C for 12 h led to formation of pentafluorobenzene and complex mixtures of samarium-containing products.

$$\underset{\mathbf{4}}{{}^1/_2[Cp^*_2Sm(\mu\text{-}H)]_2} + C_6F_5SiH_3 \rightarrow \underset{\mathbf{5}}{{}^1/_2[Cp^*_2Sm(\mu\text{-}C_6F_5)]_2} + SiH_4 \quad (4)$$

Addition of *o*-$MeOC_6H_4SiH_3$ (1 equiv) to benzene-d_6 solutions of **4** resulted in a different type of reaction. A new samarium-containing product was transiently formed, giving rise to a Cp* resonance in the ^{1}H NMR spectrum at δ 1.21, as well as dihydrogen. We believe that the samarium species is a β-methoxy-stabilized samarium−silyl complex $Cp^*_2Sm\overline{SiH_2(o\text{-}MeOC_6H_4)}$ (**7**, eq 5), on the basis of its solution IR spectrum which contains a ν_{SiH} band at 2015 cm^{-1} (for *o*-$MeOC_6H_4SiH_3$, ν_{SiH} = 2159 cm^{-1}). A shift to lower frequencies for the Si−H stretching band is associated with bonding of silicon to an electropositive center (in this case samarium).[3f,5b,27]

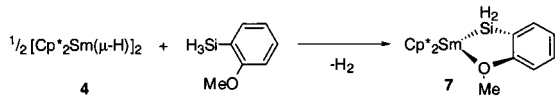

(5)

Unfortunately this Sm−Si species could not be isolated due to its decomposition in cyclohexane-d_{12} or benzene-d_6 solution, which leads to a complex mixture of samarium-containing products after 1 h. However, samarium−aryl **6** was identified as one of the products of this decomposition (24%), along with anisole (76%). Thus, the expected product of Si−C bond activation was observed, but only as the minor product of a complex reaction. The reaction of $C_6F_5SiH_3$ and **4**, on the other hand, provided a good model for the Si−C bond cleavage proposed in the pathway that proceeds through transition state **D** (Scheme 2).

The reaction of phenylsilane with **1** is not chemoselective, in that phenyl transfer (80%) and benzene formation (20%) both occur (Scheme 4). To investigate electronic effects in this transformation, we examined the reactions of **1** with $C_6F_5SiH_3$ and *o*-$MeOC_6H_4SiH_3$. When 1 equiv of $C_6F_5SiH_3$ was added to a cyclohexane-d_{12} solution of **1**, the main samarium-containing product obtained after 10 min was the robust compound **5** (85% by ^{1}H NMR spectroscopy), along with trace amounts of $[Cp^*_2SmSiH_3]_3$.[5b] This transformation was accompanied by transfer of phenyl groups to silicon, such that 0.23 equiv of $PhSiH_3$ and 0.10 equiv of Ph_2SiH_2 were also detected in solution (eq 6). Most of the phenyl groups of **1** were converted to benzene (0.42 equiv), while the remaining phenyl groups (0.15 equiv) produce $Ph(C_6F_5)SiH_2$, which gives rise to a Si−*H* triplet (J_{HF} = 8.8 Hz) in the ^{1}H NMR spectrum at δ 4.99 (the latter silane was also identified by GC−MS). Production of benzene implies initial cleavage of the Si−H bond of $C_6F_5SiH_3$ and formation of a $Sm-SiH_2(C_6F_5)$ species, which was not detected. However, such a silyl complex could react

(26) Motsarev, G. V.; Inshakova, V. T.; Kolbasov, V. I.; Rozenberg, V. R. *Zh. Obshch. Khim.* **1974**, *44*, 1053.
(27) Radu, N. S.; Tilley, T. D. *J. Am. Chem. Soc.* **1992**, *114*, 8293.

rapidly with $PhSiH_3$ or $C_6F_5SiH_3$ present in solution. The complexity of the reaction allowed only partial quantification of the silicon-containing products, and 50% of these products are unaccounted for due to the formation of insoluble $[Cp^*_2SmSiH_3]_3$ and untractable materials. Analysis of the observed reaction products, however, allowed for a comparison of the extent of Ph-transfer to silicon versus H-transfer to the phenyl group, which are roughly equal. Thus, 0.48 equiv of the phenyl groups of **1** are converted to $PhSiH_3$, Ph_2SiH_2, and $Ph(C_6F_5)SiH_2$, while 0.42 equiv of the phenyl groups give rise to benzene (eq 6).

$$\underset{\mathbf{1}}{{}^1/_2[Cp^*_2SmPh]_2} + C_6F_5SiH_3 \rightarrow \underset{\boldsymbol{5}}{0.42[Cp^*_2Sm(\mu\text{-}C_6F_5)]_2} + 0.42\ PhH + 0.23PhSiH_3 + 0.10Ph_2SiH_2 + 0.15Ph(C_6F_5)SiH_3 \quad (6)$$

In the case of *o*-$MeOC_6H_4SiH_3$, addition of 1 equiv to cyclohexane-d_{12} solutions of **1** resulted primarily in protonation of the phenyl ligand (71% by ^1H NMR spectroscopy) with concomitant formation of the Sm−silyl complex **7** shown in eq 5 (45%) after 10 min. Among the products identified from the complex reaction mixture were the Sm−aryl complex **6** (37%), Ph(*o*-$MeOC_6H_4$)SiH_2 (0.1 equiv by ^1H NMR and GC−MS) and anisole (0.1 equiv). The presence of the methoxy group seems to direct reaction toward the β-methoxy-stabilized silyl complex, and a very small amount of phenyl transfer to the silicon center is observed.

Conclusions

In synthesizing $[Cp^*_2SmPh]_2$ (**1**), we discovered an intramolecular C−H activation that leads to the formation of $Cp^*_2Sm(\mu\text{-}1,4\text{-}C_6H_4)SmCp^*_2$ (**3**) and benzene in chemistry that is analogous to that observed with related Sc[1d] and Lu[15] phenyl systems. Two pathways involving the C−H activation of a Cp* ring and a phenyl group, respectively, were identified for the thermal decomposition of **1**. This behavior is analogous to that observed for benzene activation by $[Cp^*_2LuMe]_2$.[1a] In both cases an equilibrium between monomeric and dimeric species seems to be present, with the former being responsible for the σ-bond metathesis chemistry. Such monomeric lanthanide hydrocarbyls can react following two pathways: a unimolecular one involving rate-limiting C−H activation of a Cp* ligand, and a bimolecular one involving rate-limiting C−H activation of the substrate (benzene or Cp^*_2SmPh). The first pathway exhibits no kinetic isotope effect, but the second pathway is characterized by a large isotope effect, as expected for C−H activation of benzene or Cp^*_2SmPh in the rate-limiting step. The two competing pathways lead to a concentration-dependent kinetic isotope effect arising from the relative contributions of the two reaction manifolds at different concentrations. In Watson's Lu system, the bimolecular mechanism dominates the σ-bond activation chemistry, whereas in our Sm system the two components are of comparable magnitude at the initial concentrations of **1** investigated.

In further studies, it was possible to show that phenyl-group transfer from **1** to phenylsilane is preferred over hydrogen transfer from phenylsilane (or dihydrogen) to the phenyl group of **1** (4:1 ratio) and that **1** is a feasible intermediate in the $[Cp^*_2Sm(\mu\text{-}H)]_2$-catalyzed redistribution of phenyl groups at silicon. Since **1** proved to be unstable, the isolable samarium−aryl complexes $[Cp^*_2Sm(\mu\text{-}C_6F_5)]_2$ (**5**) and $[Cp^*_2Sm(\mu\text{-}o\text{-}MeOC_6H_4)]_2$ (**6**) were independently prepared. These compounds provide further evidence that Sm−aryl complexes are viable intermediates in lanthanide-mediated transformations of arylsilanes.

The arylsilane σ-bond activation chemistry is very sensitive to the electronic effects of the substituents on the aryl groups, such that reaction of the samarium hydride **4** with $C_6F_5SiH_3$ resulted in clean Si−C bond cleavage. This transformation represents a remarkable example of a system with a Si−C bond that is more reactive than Si−H bonds. Thus, polarized $Si^{\delta+}-C^{\delta-}$ bonds such as that of $C_6F_5SiH_3$ are particularly susceptible to activation by metal hydride complexes. The electron-withdrawing ability of the C_6F_5- group gives rise to an electrophilic silicon center that is readily attacked by samarium hydride **4**. In addition, Si−C bond cleavage results in formation of a robust Sm−C bond in complex **5**. In contrast, reaction of **4** with *o*-$MeOC_6H_4SiH_3$ resulted in quantitative Si−H activation. Exclusive activation of an Si−H bond in *o*-$MeOC_6H_4SiH_3$ is favored by formation of a five-membered metallacycle $Cp^*_2SmSiH_2(o\text{-}MeOC_6H_4)$ (**7**), which is stabilized by the samarium−oxygen interaction. In addition, the electron-rich *o*-$MeOC_6H_4-$ group makes the silicon center of *o*-$MeOC_6H_4SiH_3$ the least electrophilic in the series $C_6F_5SiH_3 > PhSiH_3 > o\text{-}MeOC_6H_4SiH_3$. The intermediate electrophilicity of $PhSiH_3$ results in competitive Si−C (redistribution) and Si−H (dehydrocoupling) bond activation in reactions with **4**. The electron-rich silicon center of *o*-$MeOC_6H_4SiH_3$ is apparently not readily attacked by **4**, resulting in quantitative Si−H activation and no Si−C activation.

Phenyl-group transfer from **1** to arylsilanes appears to also be sensitive to electronic effects, as reactions of **1** with $C_6F_5SiH_3$ led to competing phenyl transfer and phenyl protonation (approximately 1:1). The lack of selectivity for Si−C versus Si−H activation in this process likely arises from the presumably weaker Sm−Ph bond relative to the Sm−H bond of **4**,[28] and the lower relative nucleophilicty of Sm−Ph. Phenyl-group transfer from **1** to the silicon center of *o*-$MeOC_6H_4SiH_3$ was minimal, accounting for only 10% of the identified silicon-containing products. Predominant Si−H activation in this reaction is apparently favored by the directing effect of the methoxy-substituted arylsilane. The greater extent of phenyl transfer from **1** to $C_6F_5SiH_3$ and $PhSiH_3$ versus *o*-$MeOC_6H_4SiH_3$ is also in agreement with the greater electrophilicity of the Si center of the former two, which results in more facile nucleophilic transfer of the phenyl group.

This work emphasizes the importance of electronic factors that control Si−C versus Si−H activation in organo-f-element systems. With a better understanding of these factors, synthetic efforts should allow development of more selective catalysts. Likewise, development of metal complexes with enhanced electrophilicity might lead to more active systems, as recently demonstrated in hydrocarbon−metal chemistry.[7] Future work will address additional aspects of the role of electronic and steric factors in metal-mediated Si−C and Si−H bond activations.

Experimental Section

General Considerations. Unless otherwise specified, all manipulations were performed under a nitrogen or argon atmosphere using standard Schlenk techniques or an inert atmosphere drybox. Dry, oxygen-free solvents were employed throughout. Olefin-free pentane was obtained by treatment with concentrated H_2SO_4, then 0.5 N $KMnO_4$ in 3 M H_2SO_4, followed by $NaHCO_3$, and finally $MgSO_4$. Thiophene-free benzene and toluene were obtained by pretreating the solvents with

(28) Nolan, S. P.; Stern, D.; Marks, T. J. *J. Am. Chem. Soc.* **1989**, *111*, 7844.

concentrated H_2SO_4, followed by Na_2CO_3, and $CaCl_2$. Pentane, benzene, toluene, and diethyl ether were distilled from sodium/benzophenone and stored under nitrogen prior to use, whereas benzene-d_6 and toluene-d_8 were vacuum-distilled from Na/K alloy. Cyclohexane-d_{12} and methylcyclohexane-d_{14} were vacuum-distilled from Na and stored under nitrogen. Reagents were purchased from commercial suppliers and used without further purification unless otherwise specified. Cp^*_2Sm,[29] $[Cp^*_2Sm(\mu\text{-}H)]_2$,[30] and $C_6F_5SiH_3$[25] were prepared by literature methods. NMR spectra were recorded on Bruker AMX-300, AMX-400, or DRX-500 spectrometers at ambient temperature unless otherwise noted. Elemental analyses were performed by the Microanalytical Laboratory in the College of Chemistry at the University of California, Berkeley. Infrared spectra were recorded on a Mattson Infinity 60 FT IR instrument. Samples were prepared as KBr pellets unless otherwise noted, and data are reported in units of cm^{-1}.

Caution! All organomercurial compounds described are potentially toxic and should be handled with caution. Manipulation with protective gloves in a well-ventilated fume hood is recommended.

$[Cp^*_2SmPh]_2$ (1). A Schlenk tube equipped with a magnetic stirbar was charged with Cp^*_2Sm (**2**) (0.20 g, 0.48 mmol) and $HgPh_2$ (0.08 g, 0.24 mmol). As benzene was added (ca. 20 mL), gray, metallic mercury began to deposit on the bottom of the flask. After stirring the mixture for 12 h under argon, the volatile materials were removed under vacuum, and the orange-red mass was extracted with 15 mL of pentane, cannula-filtered and concentrated to a volume of ca. 5 mL. Cooling to −35 °C afforded orange-red crystals in 37% yield (0.09 g, 0.09 mmol). Due to its thermal instability, compound **1** could only be characterized in solution by NMR spectroscopy: ^{1}H NMR (500 MHz, cyclohexane-d_{12}) δ 0.71 (s, 30 H, Cp*), 6.84 (d, 2 H, *m*-Ph), 7.71 (t, 1 H, *p*-Ph). Solution MW: 1160 ± 120. Calcd for $[Cp^*_2SmPh]_2$: 995.92.

$Cp^*_2Sm(\mu\text{-}C_6H_4)SmCp^*_2$ (3). Orange-red crystals of **1** (0.09 g, 0.09 mmol) were left standing overnight in a vial inside an inert atmosphere box. Yellow-tan microcrystals of **3** were recovered in quantitative yield (0.08 g, 0.09 mmol): mp > 260 °C (190 °C dec). IR 2964 (s), 2903 (s), 2857 (s), 2712 (m, $\nu_{agosticCH}$), 2628 (w), 2516 (w, br), 1480 (m), 1438 (m), 1380 (m), 1343 (w), 1212 (m), 1083 (w), 1060 (w), 1022 (m), 948 (w, br), 800 (w, sh), 728 (m, sh), 675 (w, sh), 606 (w), 590 (w), 451 (m, sh). ^{1}H NMR (500 MHz, cyclohexane-d_{12}) δ 1.16 (s, 60 H, Cp*). $^{13}C\{^1H\}$ NMR (126 MHz) δ 18.87 ($C_5\mathit{Me}_5$), 119.96 (C_5Me_5), 125.86 (ipso-Ph), 128.70 (*o*-Ph). Anal. Calcd for $C_{46}H_{64}Sm_2$: C, 60.20; H, 7.03. Found: C, 60.03; H, 7.01.

$Hg(C_6D_5)_2$. To a −80 °C solution of bromobenzene-d_5 (1.50 g, 9.26 mmol) in 30 mL of diethyl ether was added a hexanes solution of 1.6 M *n*-butyllithium (5.80 mL, 9.26 mmol) via syringe. The mixture was stirred for 2 h at −40 °C and then added with a cannula to a diethyl ether slurry of $HgBr_2$ (1.67 g, 4.63 mmol) kept at 0 °C. The reaction mixture was warmed to room temperature and stirred overnight. The products were quenched with 20 mL of water, and the organic layer was isolated with a separatory funnel. The aqueous layer was washed twice with 25 mL of toluene, and the combined organic phases were dried over $MgSO_4$, filtered, and concentrated with a rotary evaporator. Cooling the concentrated solution to −35 °C afforded 0.44 g of white crystals. A second crop was obtained from the mother liquor for a combined yield of 74% (1.25 g, 3.43 mmol). $Hg(C_6D_5)_2$ was simply analyzed by ^{1}H NMR spectroscopy (benzene-d_6) to confirm the absence of resonances in the aromatic region, and its melting point was compared to that of $HgPh_2$: mp 123−125 °C (lit.[31] 122 °C).

***o*-$MeOC_6H_4SiH_3$.** To a diethyl ether solution of *o*-bromoanisole (17.0 g, 90.9 mmol) kept at −80 °C was added a hexanes solution of 1.6 M *n*-butyllithium (56.8 mL, 90.9 mmol) dropwise with an addition funnel. The mixture was warmed to −40 °C and stirred for an hour. After re-cooling to −80 °C, the solution was slowly added to a stirred, −80 °C solution of $SiCl_4$ (15.4 g, 90.9 mmol) in 50 mL of diethyl ether. After the addition was complete, the reaction mixture was allowed to reach room temperature, and then it was stirred overnight. Volatile materials were then evaporated under vacuum, and the products were extracted with 60 mL of pentane. This pentane extract was filtered and concentrated to a viscous oil. The mixtures obtained consisted of *o*-$MeOC_6H_4SiCl_3$ in 65% yield (14.2 g, 59.1 mmol) contaminated with ca. 8% of the diaryldichlorosilane $(o\text{-}MeOC_6H_4)_2SiCl_2$. ^{1}H NMR (300 MHz, benzene-d_6) δ 3.15 (s, 3 H, O*Me*), 6.26 (d, 1 H, Ar), 6.67 (m, 1 H, Ar), 7.05 (m, 1 H, Ar), 7.63 (m, 1 H, Ar). Samples obtained in this manner were employed for the synthesis of *o*-$MeOC_6H_4SiH_3$ without further purification. Thus, a 1:1 mixture by volume of *o*-$MeOC_6H_4SiCl_3$ (14.2 g, 59.1 mmol) and diethyl ether was added dropwise via addition funnel to a stirred solution of $LiAlH_4$ in 150 mL of diethyl ether over a period of 45 min. After the addition was complete, the mixture was heated to reflux and stirred for 2 h. Upon cooling to room temperature, the products were quenched with 2-propanol and then water (50 mL each), and the resulting mixture was neutralized with 3 N HCl solution. The organic phase was isolated with a separatory funnel. The aqueous layer was washed with 2 × 25 mL of diethyl ether, and the combined organic layers were dried over $MgSO_4$, filtered, and concentrated with a rotary evaporator. The clear liquid obtained was dried over CaH_2, and distilled at 124 °C under an atmosphere of nitrogen for a yield of 68% (5.52 g, 40.0 mmol). IR (benzene-d_6 solution) 3068 (w, br), 3007 (w), 2959 (m), 2937 (w), 2836 (w, sh), 2159 (s, ν_{SiH}), 1589 (m), 1573 (m), 1475 (m), 1462 (m), 1430 (m), 1297 (w), 1278 (m, sh), 1241 (s), 1181 (m), 1162 (w), 1132 (m, sh), 1086 (m), 1043 (m), 1024 (m), 940 (s), 920 (s), 798 (w), 759 (s), 661 (m), 647 (m), 504 (w, sh), 492 (w, sh). ^{1}H NMR (300 MHz, benzene-d_6) δ 3.22 (s, 3 H, O*Me*), 4.41 (s, 3 H, Si*H*$_3$), 6.40 (d, 1 H, Ar), 6.81 (m, 1 H, Ar), 7.16 (m, 1 H, Ar), 7.46 (m, 1 H, Ar). $^{13}C\{^1H\}$ NMR (126 MHz) δ 55.24 (O*Me*), 109.91 (Ar), 117.67 (Ar), 121.49 (Ar), 132.87 (Ar), 138.59 (Ar), 165.13 (Ar). ^{29}Si NMR (376 MHz) δ −64.68. Anal. Calcd for $C_7H_{10}OSi$: C, 60.82; H, 7.29. Found: C, 60.92; H, 7.49.

$Hg(o\text{-}MeOC_6H_4)_2$. A solution of *o*-methoxyphenyllithium was prepared as described for the synthesis of *o*-$MeOC_6H_4SiCl_3$ from *o*-bromoanisole (5.00 g, 26.7 mmol). The cold solution (−40 °C) was then added dropwise via cannula to a stirred slurry of $HgBr_2$ (4.80 g, 13.4 mmol) in 50 mL of diethyl ether kept at 0 °C. The suspension was allowed to warm to room temperature, and then it was stirred vigorously for 12 h. At that point the reaction mixture was quenched with 100 mL of water, and the organic phase was isolated with a separatory funnel. The aqueous phase was extracted with 3 × 25 mL of diethyl ether, and the combined organic layers were concentrated in a rotary evaporator until a white crystalline solid was obtained. Recrystallization from toluene afforded two crops of white crystals in 73% combined yield (4.03 g, 9.75 mmol). $Hg(o\text{-}MeOC_6H_4)_2$ had been prepared previously by different methods,[32] but complete characterization has not been reported. Mp 107 °C (lit.[32] 108 °C). IR 3065 (m), 3005 (m, sh), 2949 (s), 2921 (m), 2902 (m), 2827 (s, sh), 1573 (s), 1461 (s, br), 1424 (s, br), 1296 (m), 1280 (m), 1231 (s), 1179 (m), 1162 (m), 1119 (m), 1063 (s), 1026 (w), 935 (w, sh), 790 (m, sh), 756 (s), 723 (m), 568 (w, sh). ^{1}H NMR (500 MHz, benzene-d_6) δ 3.28 (s, 3 H, O*Me*), 6.68 (d, 1 H, Ar), 7.04 (m, 1 H, Ar), 7.15 (m, 1 H, Ar), 7.19 (m, 1 H, Ar). $^{13}C\{^1H\}$ NMR (126 MHz) δ 54.99 (O*Me*), 110.62 (Ar), 122.01 (Ar), 129.52 (Ar), 138.21 (Ar), 158.79 (Ar), 164.97 (Ar). Anal. Calcd for $C_{14}H_{14}HgO_2$: C, 40.53; H, 3.40. Found: C, 40.78; H, 3.64.

$[Cp^*_2Sm(\mu\text{-}C_6F_5)]_2$ (5). A mixture of **2** (0.20 g, 0.48 mmol) and $Hg(C_6F_5)_2$ (0.13 g, 0.24 mmol) was suspended in 20 mL of pentane and stirred vigorously for 2 h in a Schlenk tube. The resulting red solution was cannula-filtered into another Schlenk tube, leaving behind gray, metallic mercury. The solution was concentrated to a volume of ca. 8 mL and cooled to −35 °C. Two crops of red crystalline **5** were obtained for a total yield of 64% (0.18 g, 0.15 mmol): mp > 260 °C. IR 2964 (s), 2908 (s), 2911 (s), 2860 (s), 2726 (w), 1634 (w, br), 1596 (w), 1532 (m, sh), 1512 (m), 1487 (m), 1424 (s), 1379 (m), 1355 (w), 1311 (w), 1222 (m, sh), 1179 (w), 1068 (m), 1027 (m), 954 (w), 921 (s), 803 (w), 774 (w), 717 (w, sh), 579 (m, br), 474 (w). ^{1}H NMR (500 MHz, benzene-d_6) δ 0.19 (s, 60 H, Cp*). $^{13}C\{^1H\}$ NMR (126 MHz) δ 19.88 ($C_5\mathit{Me}_5$), 121.81 (C_5Me_5). ^{19}F NMR (376 MHz) δ −161.4 (d, 2 F, *m*-Ph), −152.0 (t, 1 F, *p*-Ph), −146.8 (s, 2 F, *o*-Ph). Anal. Calcd for $C_{52}H_{60}F_{10}Sm_2$: C, 53.12; H, 5.14. Found: C, 53.27; H, 5.24.

(29) Burns, C. J. Ph.D. Thesis, Materials and Chemical Sciences Division, Lawrence Berkeley Laboratory, University of California, Berkeley, 1987.

(30) Jeske, G.; Lauke, H.; Mauermann, H.; Swepston, P. N.; Schumann, H.; Marks, T. J. *J. Am. Chem. Soc.* **1985**, *107*, 8091.

(31) Wade, R. C.; Seyferth, D. *J. Organomet. Chem.* **1970**, *22*, 265.

(32) Kozyrod, R. P.; Pinhey, J. T. *Aust. J. Chem.* **1985**, *38*, 1155.

[Cp*$_2$Sm(μ-*o*-MeOC$_6$H$_4$)]$_2$ (6). A Schlenk tube was charged with **2** (0.20 g, 0.48 mmol) and Hg(*o*-MeOC$_6$H$_4$)$_2$ (0.10 g, 0.24 mmol). The solids were slurried in 20 mL of pentane, and the suspension was stirred vigorously for 2 h. A yellow solution was obtained, which was filtered and concentrated to a volume of ca. 8 mL. Cooling to −35 °C afforded yellow plates of **6** in 63% yield (0.16 g, 0.15 mmol): mp 209−212 °C (205 °C dec). IR 2962 (s), 2911 (s), 2857 (s), 2726 (w), 1601 (w), 1498 (m), 1440 (m), 1413 (m), 1378 (m), 1247 (m), 1125 (w), 1101 (w), 1043 (w), 1014 (w), 755 (m, sh), 578 (m), 552 (m). ^{1}H NMR (500 MHz, cyclohexane-d_{12}) δ −4.23 (s, 6 H, OMe), 0.94 (s, 60 H, Cp*), 4.65 (s, 2 H, −Ph), 6.52 (d, 2 H, −Ph), 7.63 (d, 2 H, −Ph), 8.50 (t, 2 H, −Ph). ^{13}C{^{1}H} NMR (126 MHz) δ 17.29 (C$_5$*Me*$_5$), 107.88 (OMe), 118.83 (*C*$_5$Me$_5$), 129.97 (−Ph). Solution MW: 1250 ± 120. Calcd for [Cp*$_2$Sm(μ-*o*-MeOC$_6$H$_4$)]$_2$: 1055.98. Anal. Calcd for C$_{54}$H$_{74}$O$_2$Sm$_2$: C, 61.42; H, 7.06. Found: C, 61.43; H, 7.17.

Kinetic Studies. Samples of **1** for kinetic runs were prepared by weighing the appropriate amounts of **2** and HgPh$_2$ in the drybox, dissolving in slightly less than 1 mL of methylcyclohexane-d_{14}, and filtering into a 1 mL volumetric flask. The sample was then brought to a volume of exactly 1 mL and transferred to a J-Young tube. A convenient rate of decomposition was observed at 78 ± 1 °C (as determined by calibration with an ethylene glycol standard) at initial concentrations of **1** ranging from 1.5 to 18 mM. The reaction mixtures were heated in the DRX 500 spectrometer probe and monitored by ^{1}H NMR spectroscopy over a period of 8−10 h. The concentrations of **1** and benzene were obtained by integration of the Cp* and aromatic resonances, respectively. The error in integration was estimated to be 5%.

X-ray Crystal Structure Determination of 3. A tan, rodlike crystal of approximate dimensions 0.31 × 0.05 × 0.06 mm was mounted on a glass capillary using Paratone N hydrocarbon oil and placed under a stream of cold nitrogen on a Siemens SMART diffractometer with a CCD area detector. Preliminary orientation matrix and unit cell parameters were determined by collecting 60 20-s frames. A hemisphere of data was collected at a temperature of −123 ± 1 °C using ω scans of 0.30° and a collection time of 20 s per frame. Frame data were integrated using SAINT. An absorption correction was applied using XPREP (T_{max} = 0.855, T_{min} = 0.573). The 10330 reflections integrated were averaged in point group $P2_1/n$ to yield 3927 unique reflections (R_{int} = 0.073). No correction for decay was necessary. The structure was solved using direct methods (SIR92) and refined by full-matrix least-squares methods using teXsan. The number of variable parameters was 211, giving a data/parameter ratio of 8.37. The maximum and minimum peaks on the final difference Fourier map correspond to 0.95 and −0.68 e$^-$/Å^3: R = 0.044, R_w = 0.050, GOF = 1.36. The crystallographic data are summarized in Table 1.

X-ray Crystal Structure Determination of 5. A red, rhomboidal crystal of approximate dimensions 0.15 mm × 0.08 mm × 0.05 mm was mounted on a glass capillary using Paratone N hydrocarbon oil and placed under a stream of cold nitrogen on the same Siemens SMART diffractometer. Preliminary orientation matrix and unit cell parameters were determined by collecting 60 20-s frames. A hemisphere of data was collected at a temperature of −115 ± 1 °C using ω scans of 0.30° and a collection time of 20 s per frame. Frame data were integrated using SAINT. An absorption correction was applied using XPREP (T_{max} = 0.959, T_{min} = 0.828). The 12182 reflections integrated were averaged in point group $P\bar{1}$ to yield 8593 unique reflections (R_{int} = 0.031). No correction for decay was necessary. The structure was solved using direct methods (SIR92) and refined by full-matrix least-squares methods using teXsan. The number of variable parameters was 577, giving a data/parameter ratio of 8.12. The maximum and minimum peaks on the final difference Fourier map correspond to 2.86 and −0.53 e$^-$/Å^3: R = 0.040, R_w = 0.060, GOF = 1.66. The crystallographic data are summarized in Table 1.

Acknowledgment is made to Professor Richard Andersen for useful discussions and a generous gift of Hg(C$_6$F$_5$)$_2$, and to the National Science Foundation for their generous support of this work.

Supporting Information Available: Tables of crystal, data collection and refinement parameters, atomic coordinates, bond distances, bond angles, and anisotropic displacement parameters for **3** and **5**; kinetic plots and data (PDF). This material is available free of charge via the Internet at http://pubs.acs.org.

JA011472W